Journal of Medicinal Chemistry Article

J. Med. Chem. **2010,** *53,* 4891–4905 **4891**
DOI: 10.1021/jm100488w

Complementarity Between a Docking and a High-Throughput Screen in Discovering New Cruzain Inhibitors†

Rafaela S. Ferreira,[‡,§,∥] Anton Simeonov,*[,⊥] Ajit Jadhav,[⊥] Oliv Eidam,[§] Bryan T. Mott,[⊥] Michael J. Keiser,[§] James H. McKerrow,[∥] David J. Maloney,[⊥] John J. Irwin,[§] and Brian K. Shoichet*[,§]

[‡]*Graduate Program in Chemistry and Chemical Biology,* [§]*Department of Pharmaceutical Chemistry, and* [∥]*Sandler Center for Basic Research in Parasitic Diseases, University of California San Francisco, California 94158, and* [⊥]*NIH Chemical Genomics Center, Bethesda, Maryland 20892-3370*

Received February 3, 2010

Virtual and high-throughput screens (HTS) should have complementary strengths and weaknesses, but studies that prospectively and comprehensively compare them are rare. We undertook a parallel docking and HTS screen of 197861 compounds against cruzain, a thiol protease target for Chagas disease, looking for reversible, competitive inhibitors. On workup, 99% of the hits were eliminated as false positives, yielding 146 well-behaved, competitive ligands. These fell into five chemotypes: two were prioritized by scoring among the top 0.1% of the docking-ranked library, two were prioritized by behavior in the HTS and by clustering, and one chemotype was prioritized by both approaches. Determination of an inhibitor/cruzain crystal structure and comparison of the high-scoring docking hits to experiment illuminated the origins of docking false-negatives and false-positives. Prioritizing molecules that are both predicted by docking and are HTS-active yields well-behaved molecules, relatively unobscured by the false-positives to which both techniques are individually prone.

Introduction

Both structure-based (docking) and HTS[a] campaigns can evaluate millions of compounds as potential lead ligands for drug discovery and, increasingly, chemical biology.[1,2] Whereas all compounds are tested in an HTS campaign, only a few prioritized compounds are experimentally tested in a docking campaign. Docking is subject to well-known problems, including under-sampling protein and ligand configurations and the use of approximate scoring functions, and may thus miss many ligands. Conversely, most HTS hits are typically artifacts or problematic compounds, and winnowing these down to the few truly interesting active molecules demands much effort.

It is conceivable that the two techniques might complement each other. Docking's weaknesses[3] are orthogonal to those of HTS, and one might expect that molecules that both fit well into a protein structure, as revealed by docking, and that are active in an HTS campaign, may be the best to prioritize for initial consideration. If that is the case, one could imagine a combined approach that would dramatically increase the compounds available for evaluation to docking while improving one's ability to rapidly prioritize hits from HTS. However, it remains uncertain whether such an approach is pragmatic. Whereas there have been several comparisons of hit rates between docking and HTS,[4−9] only rarely has this been done on exactly the same compounds[4,6] and only once have the mechanism of action of all hits been evaluated.[4,10] This last study, although revealing, involved a relatively small library of compounds (70000) and found no true reversible hits by HTS, vitiating a full evaluation of the docking screen.

We therefore wished to comprehensively compare a docking and HTS campaign against exactly the same compounds and exactly the same target, systematically analyzing the mechanism of action of all active molecules and identifying those that were specific, novel, and competitive. A 197861-compound library was screened against the X-ray structure of the thiol protease cruzain, a key drug target for Chagas' disease,[11] using docking. Subsequently, the same library was screened by quantitative HTS (qHTS)[12] against this enzyme in a biochemical assay. Each compound was screened in seven point dose−response, varying from 3.7 nM to 57.5 μM, with screening statistics that supported the reliability of the screen (e.g., the Z' for the detergent free and detergent-present screens were 0.78 and 0.93, respectively).[13] To control for one of the major mechanisms of artifactual inhibition, all compounds at all concentrations were counter-screened in the presence of a nonionic detergent, and active molecules were subsequently tested in a secondary counter-screen for promiscuous covalent inhibition. All active molecules that remained were subsequently evaluated in detailed cheminformatics and mechanistic studies, ultimately including protein crystallography; the results of these evaluations are presented within.

This study enables us to pose the following questions. First, what are the HTS and the docking false positives, and what are their mechanistic bases? Understanding these mechanisms is useful in itself, and a comprehensive analysis of them, on a

†PDB ID: 3KKU.

*To whom correspondence should be addressed. For B.K.S.: phone, (415) 514-4126; fax, 415-514-4260; E-mail, shoichet@cgl.ucsf.edu. For A.S.: phone, (301) 217-5721; E-mail, asimeono@mail.nih.gov.

[a] Abbreviation: HTS, high-throughput screen; qHTS, quantitative HTS; MLSMR, Molecular Libraries−Small Molecule Repository; LC/MS, liquid chromatography/mass spectrometry; MMTS, *S*-methyl methanethiosulfonate; DTT, dithiothreitol.

Published on Web 06/11/2010

Table 1. Sources of Actives in qHTS and Docking Screen

qHTS		virtual screening	
16221 hits (100%)		198 top ranking compounds (100%)	
false positives	**16078 (99.1%)**	**false positives**	**193 (97.5%)**
aggregators	14243 (87.8%)	conformer focusing	106 (53.5%)
detergent-resistant nonselective	745 (4.6%)	*high internal energy conformations*	*101 (51.0%)*
		floppy compounds	*5 (2.5%)*
detergent-resistant weak	550 (3.4%)	high molecular weight, unfulfilled polar groups	68 (34.3%)
detergent-resistant fluorescent	507 (3.1%)	others	19 (9.6%)
others	33 (0.2%)		
noncovalent competitive	**146 (0.9%)**	**noncovalent competitive**	**5 (2.5%)**
substrates	88 (0.54%)	substrates	3 (1.5%)
inhibitors	58 (0.36%)	inhibitors	2 (1.0%)

large scale, has few precedents. Doing so is essential to meaningfully compare structure-based and high-throughput screening. Second, what are the docking false negatives and why are they missed? Because we can crystallize at least some of the new ligands with cruzain, we can investigate this question at atomic resolution. Third, can novel and reversible inhibitors be discovered for cruzain, a target that has, until now, been dominated by irreversible, covalent molecules?[11,14] Finally, can docking reliably prioritize the true inhibitors among its very top-ranked molecules? If docking can prioritize hits to test from screening, providing a structural model that bolsters the HTS readout while remaining orthogonal to it, it suggests a general method to combine the two techniques to their mutual benefit.

Results

Database Ranking by Docking. Prior to experimentally screening the MLSMR by qHTS, the exact same library was docked against a crystal structure of cruzain (PDB code 1AIM[15]). Waters and ligands were removed from the structure. The MLSMR library was prepared according to the ZINC[16] database protocols and screened using DOCK 3.5.54.[17,18] The cruzain structure was kept rigid, and ligand flexibility was considered by docking a precalculated database of conformations for each compound. Each small molecule was evaluated in up to 600 conformations, in an average of 18735 orientations (over 10 million configurations per molecule), and scored by van der Waals and electrostatics complementarity, using AMBER and DelPhi derived potentials, respectively, corrected for ligand desolvation. The best scoring pose for any given molecule was used for ranking the database.

Preliminary Characterization of HTS Hits. We previously characterized those molecules from the qHTS that could be rapidly identified as artifacts.[13] Two screens were run in parallel, one in the presence of 0.01% Triton X-100 and one without detergent. All other conditions were maintained except that the enzyme concentration was 2-fold higher in the nondetergent screen owing to the reduced activity of cruzain in the absence of detergent. In the discussion that follows, we use the term "hit" contingently, beginning most permissively, so as to reduce false negatives, and with increasing stringency as we seek to remove false positives. "Hits" were initially defined as those compounds that showed over 40% inhibition at the highest concentration assayed. By this criterion, over 16000 hits, representing approximately 8% of the whole library, were observed. Such high hit rate is not in itself credible, and our first task was to understand the origins of these molecules and winnow them down. Close to 90% were removed based on detergent-sensitive activity; that is, they inhibited strongly in the screen that lacked detergent but inhibited substantially less, and with less well-defined dose−response curves, in the screen that included detergent. This effectively reduced the apparent hit rate to about 0.8%, a level frequently encountered in screening. Another 3% of the apparent inhibitors were fluorescent artifacts.[19] Finally, the dose−response curves inherent in qHTS allowed us to reduce this number by insisting that compounds show a dose−response, and not be the product of capricious inhibition at the highest concentration, with at least 80% inhibition at the highest concentration tested. This eliminated another 3% of hits as weak inhibitors (Table 1), leaving us with 921 "hits" (6% of the original apparent "inhibitors", 0.46% of the MLSMR). Of these, 493 were "filtered inhibitors",[13] here we decided to pursue all 921 compounds that had not been removed as screening artifacts in the initial, high-throughput tests.

Characterization of these 921 compounds for detailed mechanism, and comparison to the docking results, was thus the point of departure for this study. We adopted two parallel tracks, one investigating the mechanism of compounds active by qHTS *and* that had high docking ranks, the second one pursuing compounds based on chemotype clustering and behavior in the initial qHTS. Initial testing of compounds prioritized by docking was conducted at UCSF, while initial testing of representative cluster compounds was initially conducted at the NCGC. Whereas there was some overlap among the compounds prioritized by the two criteria, there were also a substantial number of compounds that were unique to each track. All compounds that were ultimately deemed to be competitive and reversible inhibitors were subject to the same battery of confirmatory experiments.

Prioritization of HTS Follow up Based on Docking Results. We began the follow up of the remaining 921 qHTS actives by investigating those among the top ranking 1% compounds by docking. Thirty-four of these ranked among the top 1% of compounds by docking score, 19 of which could easily be resourced from vendors. These were tested in a series of low throughput assays to probe their mechanism of action. To investigate whether they were time-dependent, a hallmark of covalent-acting molecules, cruzain inhibition after 10 min preincubation with an inhibitor was compared to activity without preincubation. Two compounds showed time-dependence (Supporting Information Table S1).

Next the compounds were evaluated for colloidal aggregation in a greater detail. Even though these compounds were not detergent-sensitive in the qHTS, as usually observed for this class of artifacts, some aggregators can still inhibit enzymes in 0.01% Triton X-100, and sometimes 0.1%

Table 2. qHTS Hits Prioritized for Follow up Based on Their Ranking among Top 1% of Dock Ranked Database and Confirmed As Competitive Inhibitors

Compound structure	DOCK rank	IC_{50} against cruzain (μM)
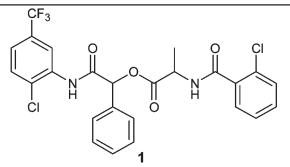 **1**	6	11
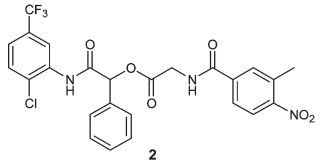 **2**	20	0.4
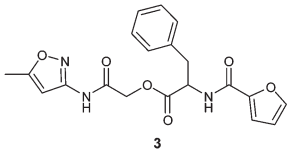 **3**	97	38
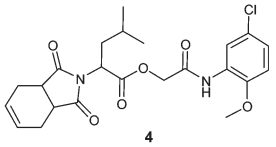 **4**	153	1
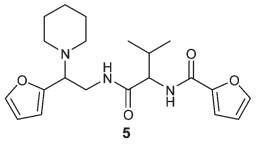 **5**	173	7
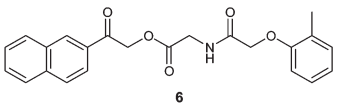 **6**	550	0.7
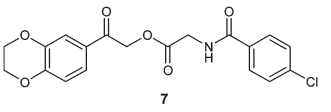 **7**	555	0.5
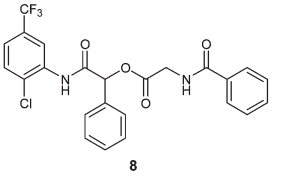 **8**	789	0.3
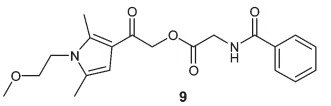 **9**	1182	18
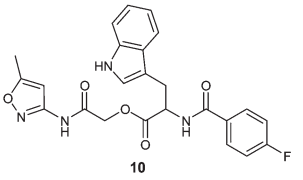 **10**	1378	3
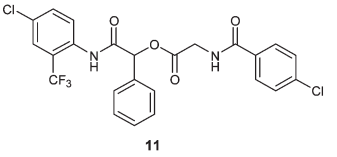 **11**	1485	0.7

of this detergent is required to prevent the nonspecific inhibition.[4] On the basis of comparison of the levels of cruzain inhibition by these compounds in three different Triton concentrations (no Triton, 0.01% and 0.1%), three compounds were classified as detergent-sensitive, likely active via colloidal aggregation, and were therefore discarded from further consideration. The compounds were also tested against AmpC β-lactamase, an unrelated enzyme, as a control for promiscuous inhibition, and two additional compounds inhibited this enzyme at concentrations inhibitory for cruzain.

This left 11 compounds that showed no detergent sensitivity, no AmpC inhibition, and no time-dependence (Table 2). Except for compounds **4** and **5**, all others can be clustered based on their 2D structure, and will be referred to as Cluster 1 from now on. The mechanism of inhibition was evaluated for one compound from each of these chemical classes, and these three scaffolds were confirmed as pure competitive inhibitors. In Cluster 1, the best scoring compound ranked 6 out of 197861 by docking, and the most potent compound of this class, with a K_i = 65 nM, ranked 789. Compounds **4** and **5**, with K_i values of 1.6 and 6 μM, ranked 153 and 173 out of the over 197000 compounds docked. Three close analogues of compound **4** were indentified among the qHTS hits. These were also retested and confirmed as inhibitors. The most potent compound in this cluster was shown to be competitive and slightly more potent than **4**, with a K_i of 0.8 μM (Supporting Information Table S2, Figure 1). Thus, each of these three classes had representatives among the 198 top scoring compounds (top 0.1% of the dock ranked library).

Characterization of HTS Hits Based on Chemotypes. In parallel with testing compounds that scored well by docking and were active in the qHTS, we sought compounds based purely on qHTS activity that represented major chemotypes of hits; the two ways of prioritizing compounds were kept intentionally separate. A combination of cheminformatics analysis and enzymological characterization was used. Visual inspection of the structures of the most active, nonfluorescent, detergent-insensitive actives suggested that many were electrophilic and thus possibly subject to attack by the nucleophilic cruzain. To facilitate identification of covalent inhibitors, these compounds were clustered based on their 2D structure and representatives from each cluster were counter-screened against papain, a cysteine protease whose substrate specificity differs from that of cruzain. The 921 top screening "hits" were represented by 199 compounds, corresponding to 47 clusters and 35 singletons; it was these 199 that were counter-screened. Of these, 167 compounds representing 38 clusters and 32 singletons had little or no specificity for cruzain over papain, consistent with a nonspecific

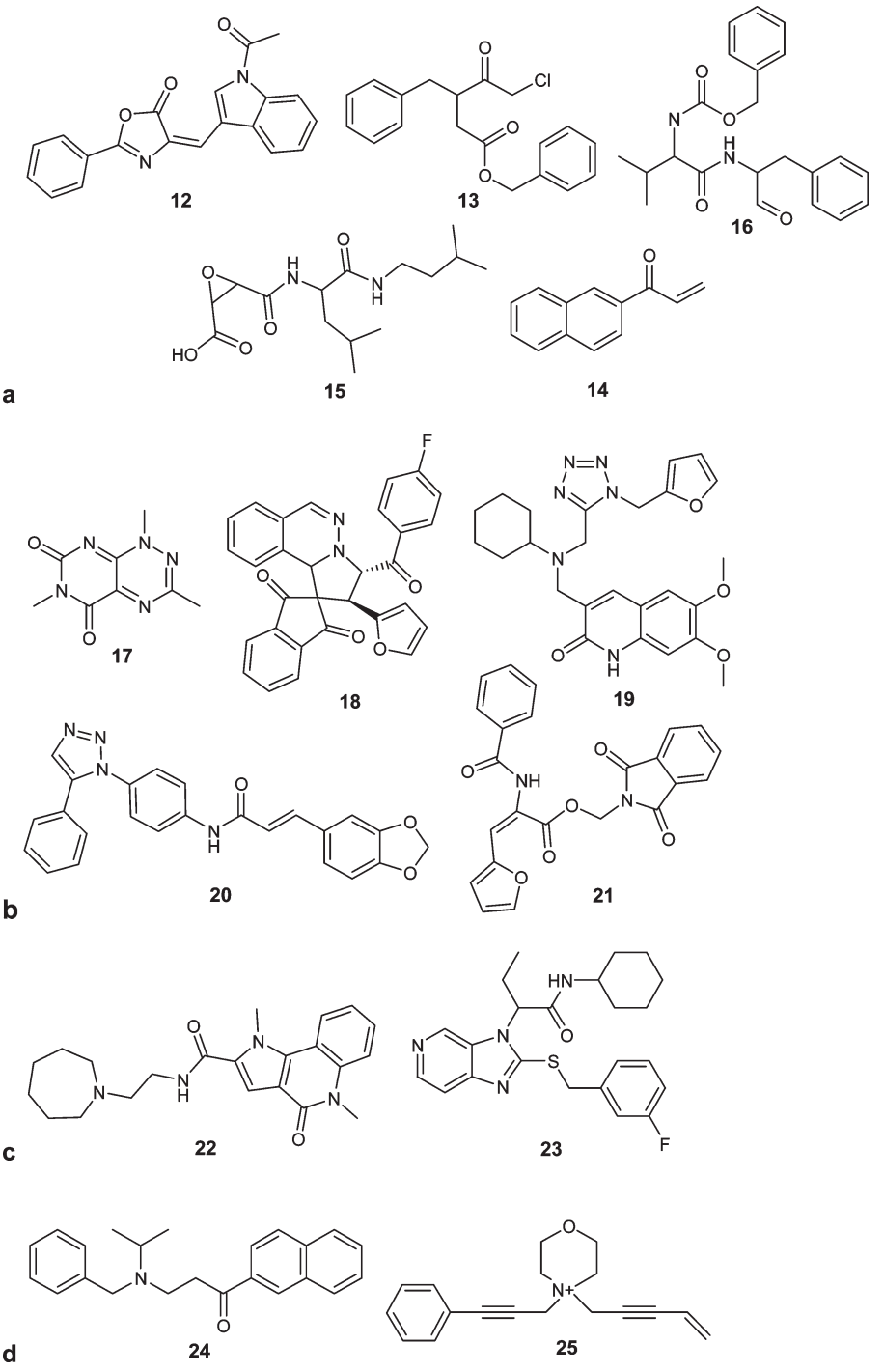

Figure 1. Compounds representative of clusters active against papain (a) and of clusters of compounds selective for cruzain and followed up after the papain counter-screen: (b) time-dependent, (c) detergent-sensitive, and (d) weak or irreproducible cruzain inhibitors.

covalent mechanism of action. Whereas papain inhibition is not definitive proof of such a mechanism, inspection of the chemical structures of these inhibitors supports that view, as they are characterized by Michael acceptors, α-halocarbonyls, and other activated electrophiles known to target sulfhydryl proteases (Figure 1a).[20] This left us with nine clusters and three singletons that were selective for cruzain over papain, including Cluster 1 that had been, in parallel, tested based on prioritization in the docking screen. Expanding back the nine clusters to all the MLSMR compounds that they represented, and that showed good dose−response curves in the qHTS, led to a total of 173 compounds from the full screen; these clusters in addition to the three singletons gave a cumulative total of 176 compounds as potential inhibitors for follow-up. We note that another class of active molecules identified at this stage, the triazine nitriles, was also pursued. These molecules act by a covalent mechanism, and so were missed by docking, which only considers noncovalent complementarity. Because these molecules have been discussed previously,[21] they will not be further considered here.

Among the 12 classes of compounds selective for cruzain, compounds from cluster 1 had been shown to be competitive inhibitors (above). As with the tests of qHTS "hits"

Table 3. Scaffolds of Cruzain Competitive Ligands

Cluster number/ compounds per cluster	Cluster member confirmed to be pure competitive with substrate	Ki (μM)	Cluster member with best DOCK score	Rank (% of database)
1/88[a]	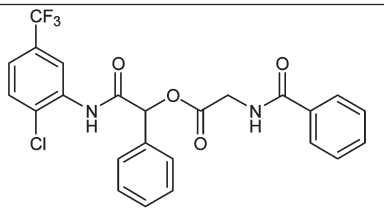 **8**	0.07	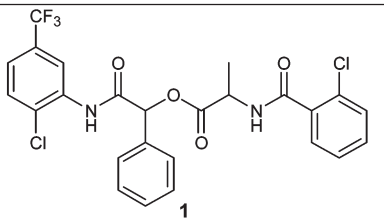 **1**	6 (0.003)
44/4	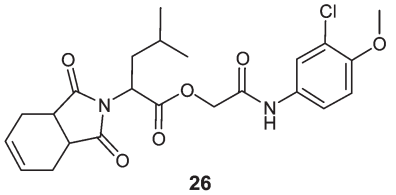 **26**	0.8	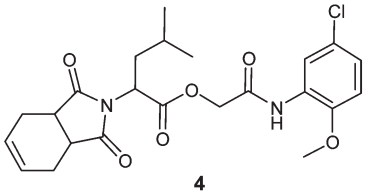 **4**	153 (0.077)
Singleton	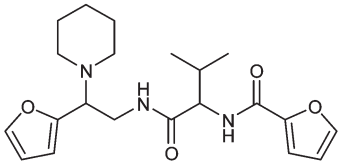 **5**	6	Same as compound tested	173 (0.087)
2/43	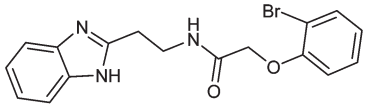 **27**	2	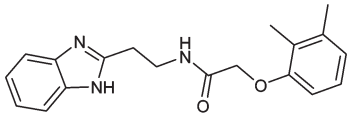 **28**	7,560 (3.82)
31/10	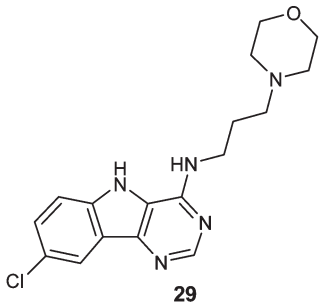 **29**	2	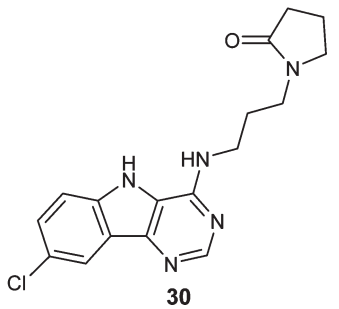 **30**	31,359 (15.85)

[a] This class of ligand is recognized as a substrate of cruzain; all others are inhibitors.

prioritized by their docking rank (above), the remaining 11 compound clusters were tested for time-dependence, detergent-sensitivity, promiscuous inhibition, and mode of inhibition. Five of these 11 classes of molecules were found to be time-dependent (Figure 1b, Supporting Information Table S3). Of these, three were Michael acceptors and one was an activated thiol ether, chemotypes that one might expect to be reactive against cruzain's activated thiol nucleophile. We inferred that these five clusters, representing 16 of the 176 compounds (Supporting Information Table S3), were covalent-acting inhibitors and so they were not further pursued. Of the remaining six scaffolds, two apparently selective chemical classes were classified as detergent-sensitive, at the higher detergent concentration, and discarded (Figure 1c). For two of the four chemical classes that were neither time-dependent nor detergent-sensitive, inhibition was weak or not observed on detailed replication, including resourcing the compound from vendors; these were also discounted (Figure 1d). The remaining two classes were tested against AmpC β-lactamase and did not inhibit this enzyme (Supporting Information Table S3). Finally, these compounds were tested at several substrate and compound concentrations and confirmed as reversible, competitive inhibitors (Supporting Information Figure 1), with K_i of 2 μM in both cases (Table 3). Because these two chemical scaffolds were not represented among the top ranking 0.1% or even among the top 1% of the dock ranked database, these classes are docking false negatives.

In summary, after detailed testing, five classes of compounds, representing 146 compounds and 0.07% of the library, were identified as competitive, reversible ligands for cruzain (Table 3, Supporting Information Figure 1).

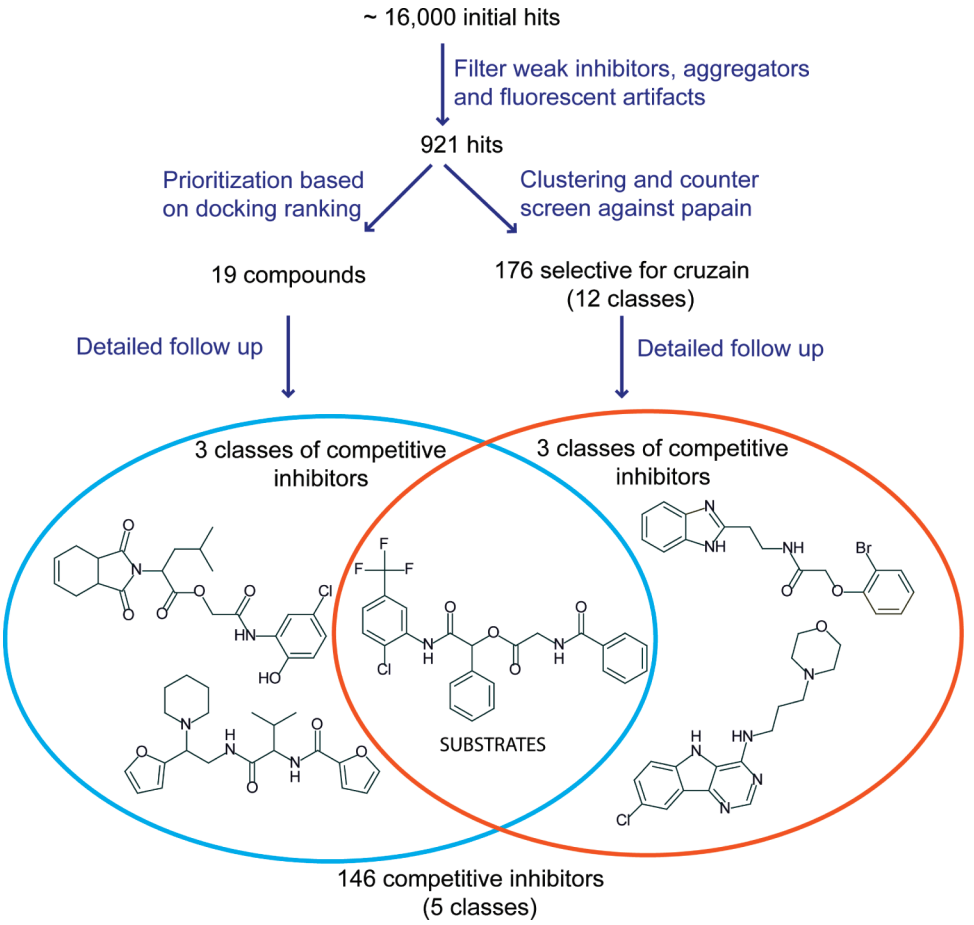

Figure 2. Two parallel strategies employed in the follow up of qHTS hits. After removal of aggregators, fluorescent artifacts, and weak inhibitors, the remaining HTS hits were followed up either based on docking prioritization or based on clustering by chemotypes.

Of these five, two were identified only by the chemotype-based follow-up pursued without reference to docking rank; these two classes are docking false negatives. Correspondingly, another two of the five classes were only pursued because they had, in fact, high docking ranks. It was not pragmatic to follow up each of the 921 "hits" in the papain counter-screen, and some compounds were necessarily left out: these two, one of which represents a cluster of only four compounds and the other which is a singleton, were among them. Whereas they are certainly not screening false negatives, as they were active in the qHTS, it is likely they would not have been prioritized for follow up absent the docking results. Finally, a fifth cluster, representing the vast majority of hits, was prioritized for follow-up based both on high docking rankings and chemotype clustering (Figure 2). In total, these 146 compounds represent 1% of all the initial "hits" and 13% of the detergent-resistant counter-screened hits.

Search for HTS False Negatives. When combined with HTS, virtual screening may not only prioritize HTS hits, but in principle it can also illuminate HTS false negatives. Indeed, in a docking and HTS campaign against β-lactamase, the docking screen identified just such false negatives.[4] To search for possible HTS false negatives for cruzain, we therefore repurchased and retested compounds inactive in the qHTS that had good complementarity to cruzain by docking. Ultimately, 32 such compounds were selected and retested. Among these, eight inhibited cruzain between 40 and 70% at 200 μM (Supporting Information Table S4). However, further confirmation of these was complicated by solubility limits. Whereas these compounds were neither time-dependent nor detergent-sensitive, full establishment of their mode of inhibition and reliability was not possible. Given their weak activity, they were therefore disregarded; no HTS false negatives were reliably identified despite substantial effort.

Comparison between Docking and HTS Results. To quantify DOCK performance in predicting HTS results we turned to enrichment factors, which compare the observed performance to what would be expected if the database was randomly ranked. A commonly used metric to evaluate virtual screening, the enrichment factor is given by the ratio between the percentage of ligands found in a chosen percentage of the database and the percentage of the database evaluated. For instance, if 100 known ligands are included among a larger library of compounds docked to a target, and 8% of the ligands rank in the top 1% of the overall database of compounds, an enrichment factor of 8 is obtained because it is expected that only 1% of the ligands would be found by random selection in this slice of the database. This is given by the following formula:

$$\mathrm{EF}_{(\%)} = \frac{N_{\mathrm{active}(\%)}/N_{\mathrm{active}}}{N_{(\%)}/N_{\mathrm{total}}}$$

Where $\mathrm{EF}_{(\%)}$ is the enrichment factor at a chosen percentage X of the database, $N_{\mathrm{active}(\%)}$ is the number of actives ranked among the top X of the database, N_{active} is the total number of actives in library, $N_{(\%)}$ is the total number of

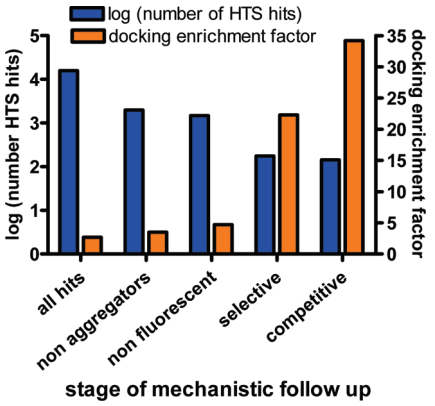

Figure 3. Progression of the number of HTS hits and docking enrichment factors at different stages of mechanistic follow up. The enrichment factor was calculated at the top 0.1% of the database (198 compounds) and represents the ratio between the percentage of ligands ranked among these compounds and the percentage which would be expected to be found by random chance (0.1%).

compounds in X, and N_{total} is the total number of compounds in the library.

On the basis of this metric, we observe a significant improvement of DOCK performance as the HTS hits are progressively winnowed and confirmed (Figure 3; see also Supporting Information Figure 2 for full enrichment curves). Here we focused on the top 0.1% of the database, or the 198 top-ranking compounds, which is to say the very top of the ranked database. The initial enrichment factor, if all HTS hits are considered as valid, is 3-fold over random selection. As artifacts and covalent inhibitors are eliminated and we progressively consider only nonaggregating, selective, and competitive inhibitors, enrichment increases to 4-, 22-, and 34-fold. The largest increase is obtained when covalent inhibitors are eliminated, reflecting the modeling of noncovalent complementarity in docking and its disregard for reactive functionality. The improvement in enrichment upon eliminating aggregators is modest. This was initially unexpected, because one might imagine that this is an artifact unique to HTS. However, the tendency to aggregate is correlated with molecular weight, as is docking score, and so docking also often enriches what are ultimately shown to be colloidal aggregators (the original molecules shown to act by this mechanism were, in fact, discovered from a docking screen[5,22]).

Among the top 198 hits by DOCK ranking (0.1% of the database), five competitive cruzain ligands were found, one of them ranking sixth among all 197861 compounds. This and another two compounds, ranking 120 and 197, belonged to HTS cluster 1 (Table 3). The other two compounds successfully predicted, **4** and **5**, ranked 153 and 173, respectively. These molecules represent three out of five competitive scaffolds found by HTS. If we consider all hits which ranked in the top 1% of the docking screen (i.e., top 1980 molecules), another 11 representatives of cluster 1 were found, including the most potent cruzain inhibitor found in this screen, compound **8**, with a K_i of 65 nM and rank 789. The other two scaffolds, clusters 2 and 31, scored poorly by DOCK and are therefore considered here as false negatives, with their best scoring compounds respectively ranking 7560 (3.8% of the database) and 31359 (15.9% of the database). The predicted binding modes for the best scoring compounds in each chemical class are shown in Figure 4. In most cases, hydrogen bonds or dipole−dipole interactions are observed to Gly66, Asp161, and Gln19, as previously observed in published crystallographic complexes of cruzain bound to other inhibitors.[23]

Among the clusters of competitive ligands, cluster 44 showed the best enrichment, with its best scoring compound (compound **4**) ranking 153 and the worst scoring compound ranking 21010 (10.6% of the database) (Supporting Information Table S2, Figure 2b). Comparing the enrichment curves for clusters 1, 2, and 31, it was surprising to observe that virtual screening performed better for cluster 1, the most flexible class of compounds (Supporting Information Figure 2b). Within cluster 1, we investigated whether there was any correlation between the relative ranking of the molecules and their physical properties, especially the number of rotatable bonds. However, for the properties analyzed (number of rotatable bonds, molecular weight, xlogP, polar surface area, number of H-bond donors or acceptors), no trends were observed.

Interested in better understanding docking artifacts, the false positives among the 198 top scoring compounds by docking were visually inspected. These compounds are characterized by two principal features: molecules containing several polar groups with unfulfilled cruzain interactions and molecules with high internal energy (Table 1, Figure 5). These observations reflect known liabilities of the docking program used here, DOCK 3.5.54,[17,18] and are common problems in the field.[24,25] The observation of groups with many unfilled interactions, responsible for 34% of these false positives, is likely caused by the difficulty in balancing the positive effects of electrostatics interactions and the energetic cost of ligand desolvation. The most common source of false positives, observed for 53.5% of the top ranking compounds, were high energy conformations. Almost all cases in this class (51%) were due to conformations of back-to-back amides in which the torsional angle around the carbonyl−carbonyl bond is zero and the two amide hydrogens, both bearing a partial positive charge, point toward each other (Figure 6b). These hydrogens interact with the backbone carbonyl from Asp161 in cruzain, making favorable electrostatic interactions with the enzyme but are unpenalized for the electrostatic cost of juxtaposing the two amide nitrogen dipoles. High energy conformations that score well reflect the absence of an explicit consideration of ligand internal energy in the DOCK 3.5.54 scoring function. Whereas only the lowest energy conformations of a compound are included when building the database to be docked, molecules within a certain energy window from the lowest energy are included and differences in the internal energy among these conformations are not taken into account at later stages in the virtual screening. A related case was observed for 2.5% of false positives, which contained highly flexible substituents. These reflect the absence of a penalty for entropic losses upon binding to the protein.

Comparing Docking with Ligand-Based Screening. A goal of this project was to discover novel chemotypes to inhibit cruzain. A question that emerged in the review and revision of this project was how novel the compounds discovered were and how efficient the structure-based and HTS modalities were. To investigate this question, we used the ligand-based similarity ensemble approach (SEA),[26] which had shown some success in identifying new ligands for well-annotated targets, to screen each compound in the MLSMR

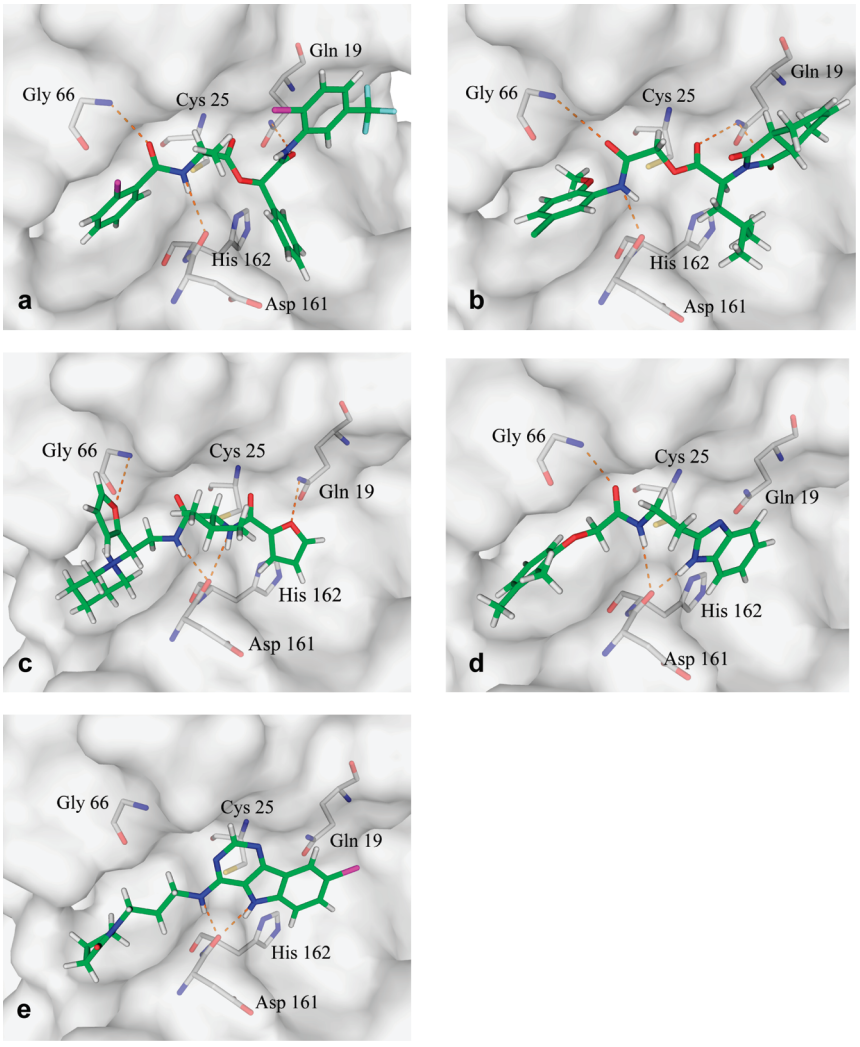

Figure 4. Predicted binding modes for competitive cruzain inhibitors. Best scoring pose of highest ranking compound in each cluster shown. (a) compound **1**, rank 6 (out of 197861), cluster 1; (b) **4**, rank 153; (c) **5**, rank 173; (d) **15**, cluster 2, rank 7560; (e) **17**, cluster 31, rank 31359. Cruzain surface shown in gray. Active site cysteine 25 and residues involved in hydrogen bond interactions shown in sticks. Dashed lines represent hydrogen bonds. Protein carbon atoms colored gray and small molecules carbon atoms colored green. Oxygen, nitrogen, and sulfur colored red, blue, and yellow, respectively. Chlorine and fluorine colored magenta and cyan, respectively. Figures prepared with Pymol.[59].

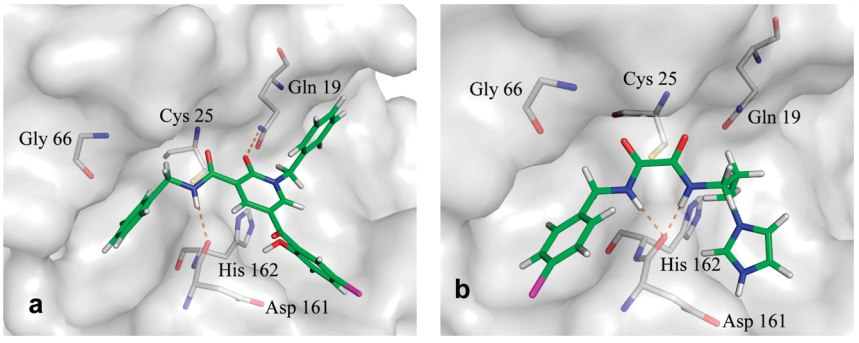

Figure 5. Main sources of virtual screening false positives. Predicted poses for top ranking false positives: (a) rank 1, illustrating presence of unfulfilled polar interactions, (b) rank 3, representing high energy conformations. Cruzain surface shown in gray. Active site cysteine 25 and residues involved in hydrogen bond interactions shown in sticks. Dashed lines represent hydrogen bonds, waters are shown as red spheres. Protein carbon atoms colored gray, and small molecules carbon atoms colored green. Oxygen, nitrogen, sulfur, and chlorine colored red, blue, yellow, and magenta, respectively. Figures prepared with Pymol.[59].

library against a set of 128 known cruzain inhibitors. Compounds were screened by 2D chemical similarity based on their ECFP4 and Daylight fingerprints. Applying an *E*-value threshold of 10^{-10}, 961 hits were obtained in former case and 154 hits in the later. Whereas some irreversible and likely nonspecific inhibitors were identified, none of the cruzain competitive inhibitors discovered in this study was identified by this ligand-based approach, even if a less stringent *E*-value

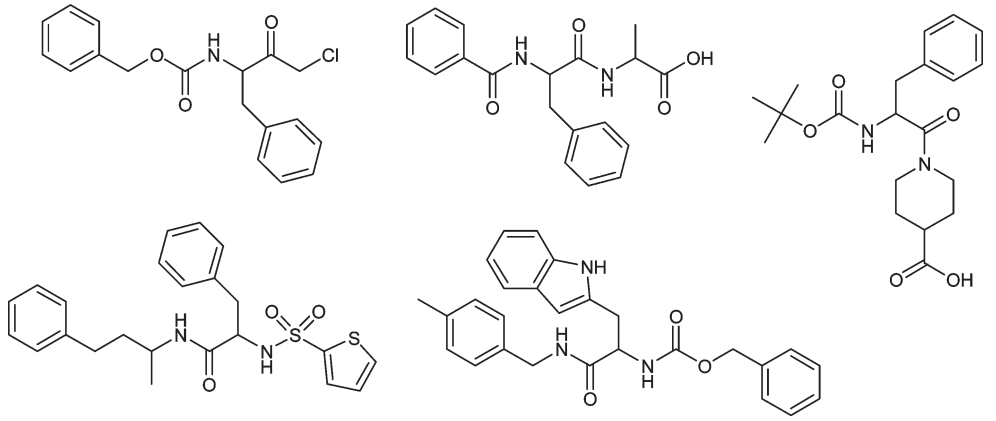

Figure 6. Chemical structures of representatives of top scaffolds identified by ligand-based virtual screening. No competitive inhibitors were among the hits identified by this method.

threshold of 10^{-1} was used. The top hits obtained were peptidic inhibitors (Figure 6) and in some cases contained reactive moieties, as expected based on the properties of most known cruzain inhibitors. These results support the view that the inhibitors discovered by docking and qHTS were substantially different from known cruzain inhibitors.

Discovery of a Class of Cruzain Substrates among Competitive Compounds. To understand the molecular bases of recognition, we pursued cocrystallization of cruzain with the noncovalent competitive inhibitors. Cruzain was cocrystallized with one compound from each class of competitive inhibitors (compounds **4**, **5**, **11**, **27**, and **29**), using standard conditions.[21] Crystals diffracted well, often to ultrahigh or near-ultrahigh resolution (1.0−1.3 Å), and the structures were determined. However, electron density for most ligands was poor, and with exception of compound **27** (cluster 2) it was not possible to resolve ligand coordinates unambiguously. Although poor electron density might be explained by poor solubility or high flexibility of compounds, the presence of labile groups, especially esters in cluster 1 and compound **4**, prompted us to investigate if compounds were degraded in the crystallization buffer (2 mM Bis-Tris pH 5.8). To this end, we applied liquid chromatography coupled to mass spectrometry (LC/MS). Most compounds were stable over several hours in the presence or absence of cruzain, however we observed enzyme-catalyzed degradation of compound **11** in the presence of 100 nM cruzain (Figure 7, Supporting Information Figure 3). While the intact compound was still observed in solution even after one day of incubation in the absence of cruzain, in the presence of enzyme it was absent after a 40 min incubation, indicating that cleavage of **11** was enzyme catalyzed. Further evidence of hydrolysis was obtained by measuring time-dependence of cruzain inhibition by two compounds from cluster 1, **11** and **8**, which showed the lowest IC_{50} against cruzain within this cluster. We compared percentages of cruzain activity after incubation with 1 μM of **8** or 10 μM of **11** from 0 to 240 min (Supporting Information Figure 3). A clear time-dependent effect on the fraction of active cruzain was observed in the presence of enzyme.

Before learning of the substrate properties of this chemotype, we investigated a limited SAR series around the benzamidoacetate series (exemplified by compounds **8** and **11**). Several analogues were prepared and evaluated for potency (Supporting Information Table S5). The most active of these new compounds inhibited cruzain with an IC_{50} of

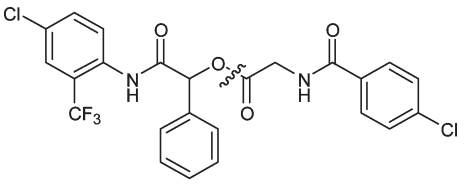

11

Figure 7. Identified cruzain substrate. Structure of compound **11**, identified as a cruzain substrate through LC/MS and biochemical assays, and highly ranked by docking. Predicted cleavage site indicated (wavy line).

30 nM, 8-fold better than that of the best HTS hit in this series, **11** (IC_{50} = 260 nM). Whereas this suggests that this series is optimizable, we note that even in these more potent, low nanomolar inhibitors, replacement of the ester functionality with an amide moiety resulted in complete loss of activity as did other hydrolytically stable ester isosteres such as oxadiazole and thiadiazole analogues (Supporting Information Figure 4). This suggests that even these more potent ligands are also best thought of as tight-binding substrates for the enzyme.

Compounds **4** and **5**, which are not from cluster 1, were also evaluated for stability in the presence of enzyme by both LC/MS and the time-dependence assay but did not behave as substrates (Supporting Information Figure 5). Over a four-hour period, or even after a day in the case of compound **5**, these compounds were stable by LC/MS in the presence of 100 nM cruzain. They also inhibited cruzain at similar levels regardless of incubation time.

Crystal Structure of Cruzain/27 Complex. A structure of the cruzain complex with compound **27**, a docking false negative, was solved to near ultrahigh resolution (1.28 Å, Table 4). Most residues in the active site are observed in conformations similar to the ones present in the cruzain structure used for docking.[15] The most significant changes are a flip in Gln159 and double conformation of the catalytic Cys25 (Supporting Information Figure 6). The lower occupancy Cys25 conformation (approximately 30%) is covalently modified by *S*-methyl methanethiosulfonate, a covalent reversible cruzain inhibitor used in the purification of this enzyme and removed prior to the crystallography. The higher occupancy Cys25 conformation is unmodified. Also, small differences are observed for residues forming the S2 pocket, such as Glu208, Leu67, and Leu160, which move toward the ligand.

Unambiguous electron density was obtained for the inhibitor (Figure 8). The amide group in **27** binds between the S1 and S2 pockets, making interactions similar to those previously observed for covalent cruzain inhibitors,[23] although the X-ray structure confirms the lack of covalent attachment. The amide nitrogen hydrogen bonds to the carbonyl in Asp161 (distance 2.99 Å), whereas the carbonyl hydrogen bonds to the backbone nitrogen in Gly66 (distance 3.04 Å). The bromo-phenyl ring occupies the S2 pocket of cruzain, and the ester makes a dipole−dipole interaction with the backbone nitrogen in His162 (3.19 Å). The benzimidazole ring is mostly solvent exposed, and its nitrogens hydrogen-bond to waters 226 and 218 (3.00 and 2.55 Å, respectively). In the docking prediction, the bromo-phenyl ring occupies the S2 pocket as experimentally observed, although the ring is flipped by approximately 180° and the amide nitrogen hydrogen bonds to Asp161 carbonyl (2.85 Å), also as observed by crystallography (Figure 8). Past this point, the overlap with the crystallographic pose becomes poor because the benzimidazole ring position is in a completely different region of the active site.

Table 4. Data Collection and Refinement Statistics for Cruzain/**27** Complex

Data Collection	
space group	$P6_522$
cell dimensions	
a, *b*, *c* (Å)	82.98, 82.98, 101.73
α, *β*, *γ* (deg)	90, 90, 120
resolution (Å)	1.28(1.33−1.28)[a]
R_{sym} or R_{merge}	9.2(18.6)
$I/\sigma I$	78.0(29.3)
completeness (%)	99.9(100.0)
redundancy	11.5(11.0)
Refinement	
resolution (Å)	41.46 to 1.28
no. reflns	59354
R_{work}/R_{free}	0.115/0.144 (0.078/0.132)
no. atoms	
protein	1,559
ligand/ion	163
water	314
B-factors	
protein	8.5
ligand/ion	12.8
water	25.7
rms deviations	
bond lengths (Å)	0.013
bond angles (deg)	1.491

[a] Values in parentheses are for highest-resolution shell.

Investigation of Causes of Poor Ranking of Compound 27 by DOCK. Upon obtaining the structure of cruzain bound to **27**, we were interested to know why DOCK failed to predict the correct binding mode for this compound. Whereas the specific reasons for virtual screening failure are hard to determine in a complex binding site, it is usually possible to divide docking problems into inadequate sampling and poor scoring.

Problems in sampling might owe to the absence of the relevant conformation in the database or to inadequate sampling of the right orientation by docking. To investigate if the crystallographic conformation was docked, all 600 conformations of **27** present in the database were rigidly docked in multiple orientations and the rmsd between the observed binding mode and the best scoring pose for each conformation was calculated. Several conformations within a 2 Å cutoff from the crystallographic were observed, with rmsd values as low as 1.4 Å (Supporting Information Figure 7). Even though the torsional angle around the methylene−carbonyl bond in this conformation differed from the crystallographic one, most of the compound overlaps well with

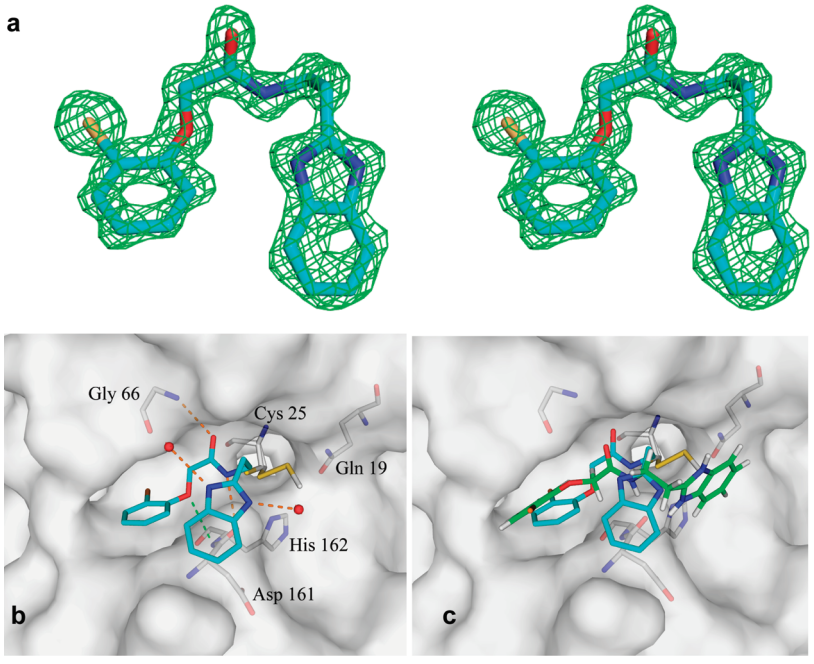

Figure 8. Comparison between docking pose and crystallographic geometry of compound **27**. (a) Stereo view of unbiased electron density ($F_o - F_c$ countoured at 3σ) from cruzain/**27** complex structure determined to 1.28 Å. (b) Key interactions between compound **27** and cruzain. Dashed lines represent hydrogen bonds (orange) or dipole−dipole interactions (green), waters are shown as red spheres. (c) Superposition of docking pose and crystallographic geometry. Carbon atoms colored gray for cruzain, cyan for crystallographic pose, and green in DOCK predicted pose. Oxygen, nitrogen, sulfur, and bromine colored red, blue, yellow, and orange, respectively. Figures prepared with Pymol.[59]

the crystallographic pose, capturing the interactions observed experimentally. This result suggested that poor ranking of this compound was not due to undersampling.

Next, we investigated whether the crystallographic pose of **27** would score well in the energy potential maps used for docking. DOCK 3.5.54 uses three terms in its scoring function: van der Waals interactions, electrostatic interactions, and a penalty for ligand desolvation[18,27,28] (M. Mysinger and B.K.S., unpublished). For any docked orientation, the contribution of each atom for each term in the scoring function can be evaluated. In the energy potential maps calculated from the conformation of cruzain used in the docking, the crystallographic geometry of **27** scores poorly at −8.5 kcal/mol and would have ranked 180479 out of the 197861 molecules docked (DOCK's energy scores are typically far offset from binding affinities, as was the case here). This is much less favorable than the energy scores obtained for the best scoring pose of this compound by docking (−35.5, rank 28521). The difference between the scores of these two conformations is due to much less favorable scores for the crystallographic conformation both in the van der Waals term (−8.4 vs −22.2 for the docked conformation) and in the balance between electrostatic score and ligand desolvation (−0.1 vs −13.3 Supporting Information Table S6). We then evaluated how **27** scored in grids prepared using the cruzain/**27** complex structure determined here but otherwise following the same protocol in grids preparation. The score of the crystallographic pose improved, and the gap between scores of crystallographic pose, −17.6 kcal/mol, and the best scoring pose by DOCK, −26.7 kcal/mol, is reduced. This improvement is due to more favorable van der Waals interactions, suggesting that even though the conformational changes observed for residues in the cruzain active site are small, considering this flexibility would substantially impact the scoring of this compound.

Discussion

We may now tender preliminary answers to the questions that motivated this study. The dominant source of false positives in this screen, as in earlier ones,[10] remains colloidal aggregation, contributing 88% of the initial screening hits in the cruzain qHTS. Contributions from fluorescence interference and promiscuous covalent inhibition, although still substantial at 3% and 5% of the initial hits, respectively, were much less. As in earlier studies,[10] the results support response to detergent as a fast initial screen to identify colloidal aggregators. Whereas this test does not identify all aggregators, it does identify over 95% of them, and as previously it appears more reliable even than properties such as high Hill slopes,[29] which only identify about 50% of aggregators,[13] also consistent with previous observations.[10] This study is also one of the few, perhaps only, to allow a comprehensive analysis of docking false positives, and here the results were perhaps less expected. The largest single group of these false positives owed to the adoption of high-energy ligand conformations that fit the cruzain structure well but, without being grossly wrong, are energetically inaccessible to the small molecules. Correspondingly, testing of the entire library reveals docking false negatives, which X-ray crystallography suggests derive from scoring problems, partially due to small conformational changes in the protein upon ligand binding. Notwithstanding these problems, this study has identified five new, competitive families of inhibitors for cruzain, four of which are noncovalent and reversible, suggesting that such inhibitors can be found despite the dominance of covalent inhibitors for this and related thiol proteases. Perhaps most generally, if most tentatively, this study supports the idea that docking and high-throughput screens are complementary and may be usefully combined, with the docking providing orthogonal structural support for the prioritization of interesting screening "hits" to follow up. We take each of these points in turn.

Owing to the high frequency of false positives in HTS and docking,[30−34] discovering true inhibitors from among initial screening hits requires extensive counter-screening and mechanistic investigation. The observations afforded by qHTS, where every compound was tested in seven point dose−response, are of relatively high quality for the field, and even so, only 1% of initial hits were noncovalent, competitive inhibitors. Whereas colloidal aggregation remains by far the dominant form of artifact,[35−37] again contributing approximately 90% of the hits,[4,10,13] this biophysical mechanism has the virtue of being easily controlled for, at least for the majority of aggregators, that are detergent sensitive. But even among the active molecules that remain after discarding the detergent-sensitive aggregators, over 90% still act by undesirable mechanisms. This is consistent with the idea that the most difficult part of a screening project comes after the screen has been performed and one is left with a large number of potentially interesting molecules, most of which are misleading, through which one must carefully sift by detailed experiment. Analyzing the direct, unfiltered results of HTS campaigns, such as one might often find in public repositories, might lead one quickly astray.

Among virtual screening top hits, approximately 90% could be explained by two main sources of false positives. Over half of these artifacts result from failing to penalize high-energy compound conformations in the docking score. This supports the need to consider an internal energy term for conformations docked and the loss of degrees of freedom for the ligand, as previously demonstrated in a study of HIV reverse-transcriptase inhibitors.[25,38] Another third of the false positives owes to high molecular weight compounds containing unfulfilled polar groups. These compounds likely score well due to difficulties in balancing the favorable van der Waals and electrostatic interactions with the protein and the unfavorable desolvation energy involved in the formation of the complex.

The determination of the crystal structure of the cruzain/**27** complex illustrates one of a docking false negative at atomic resolution. With the structure determined, it seems clear that a contribution to its low ranking in the docking screen is that in its bound form cruzain makes small but important conformational accommodations that improve its overall complementarity to the inhibitor. This reinforces the importance of considering protein flexibility in structure-based screens, even for relatively rigid active sites, like that of cruzain. This remains the subject of intense research,[39−42] and it is in some senses an expected problem. Less anticipated was the adoption of a conformation where that the benzimidazole ring of **27** climbs out of the active site. The complementarity here, also missed in the docking, is with ordered water molecules, the use of which in docking is also being pursued.[43−46] More broadly, whereas previous combinations of virtual and experimental screening have led to the identification of hits,[6−9] illustrating some of the strengths of docking, reporting the rate of docking false negatives allows a fair evaluation of virtual screening also from its failures. To our knowledge, this

has been previously reported in only one study[6] and without structural information on the binding mode of the false negatives.

An encouraging result to emerge from this study was the discovery of five new scaffolds of competitive inhibitors of this key parasitic target, with K_i values ranging from 65 nM to 6 μM. Whereas several classes of inhibitors for this enzyme have been previously described, almost all are peptidic covalent agents. Among the classes discovered here, some compounds are more peptidic, and in the case of cluster 1 were later found to be cruzain substrates. Other molecules, in clusters 2 and 31, present novel nonpeptidic scaffolds. These compounds could serve as starting points for medicinal chemistry optimization, especially clusters 2 and 31, which contain mostly lead-like[47] compounds. In the case of cluster 2, the high resolution crystal structure reported here can provide additional guidance for a structure-based design effort. Consistent with the novelty of these chemotypes, none of these five scaffolds were identified by an inference-rooted ligand-based screen, which instead suggested chemotypes that closely resembled previously known ligands and that, if anything, would act in a covalent and irreversible manner (Figure 6). Because most known cruzain inhibitors used in the reference set were high molecular weight, covalent, peptidic inhibitors, this is unsurprising. Of course, this reflects the results of only one ligand-based method, and it may well be that another such technique would have found the true ligands revealed here by docking and qHTS. Still, the failure to find the true noncovalent ligands by an inference-based approach supports the novelty of the chemotypes discovered here.

Perhaps the most ambitious goal of this study was to investigate how structure-based screening can prioritize true actives from HTS and the origins and frequency of false positives and false negatives in this approach. Even with all of the codicils, caveats, and liabilities in docking, half of the scaffolds that turned out to be noncovalent, competitive inhibitors identified by HTS, in addition to the class of substrates identified here, were among the top 0.1% of the collection prioritized by docking. Indeed, two of the five classes of ligands were only prioritized for follow-up based on their docking rankings; because these compounds represented only small clusters, they had little SAR and so were not prioritized for further investigation as part of the HTS workflow. Clearly it was *combination* of activity in the qHTS and high docking ranking that identified these compounds; we do not pretend that these represent screening "false negatives" as this term is usually understood. More broadly, had we relied on docking to prioritize compounds to be tested experimentally, rather than pursuing the parallel tracks that we did, we would have screened 1000 times fewer compounds but found 60% of the competitive scaffolds. Had we screened the top 5% docking ranked library, only one inhibitor class would have been missed. This agrees with earlier work by Keseru and colleagues, where the top ranking 1% of docked molecules resembled four of the six scaffolds found by HTS,[6] and with a β-lactamase study from our own groups, where all of the true noncovalent inhibitors from a virtual screening and HTS were identified by docking alone; both of these studies represented much smaller screens than that undertaken here.[4] This work supports the potential for using structure-based virtual screening in the prioritization of compounds either to be screened by HTS or, as is our preference, to be pursued after the HTS is prosecuted.

Experimental Section

Database Preparation. The 197861 compounds present in the MLSMR database were submitted to standard preparation protocols for addition to the ZINC database,[16] as recently described.[4] After removal of duplicates, 195177 unique molecules were detected, out of which 187693 were successfully added to the database. The discrepancy of 7484 molecules not added to the database is due to 531 compounds filtered due to egregious violation (such as molecular weight over 600 g/mol, unacceptable atom, or more than 20 chiral centers), 3151 molecules that were not handled correctly by our automatic database preparation procedure and 3802 not loaded for other reasons, such as absence of polar atoms.

Virtual Screening. The compound library was virtually screened using DOCK 3.5.54. Docking was performed against PDB structure 1AIM.[15] This structure was selected after a comparison of the 13 structures of cruzain in complex with inhibitors at that point available in the PDB. Only very small differences were observed for the active site residues conformations, except for Glu208, which is highly flexible and can be either exposed to solvent or rotated toward the cruzain S2 pocket.[48] In previous docking studies with cruzain, we were successful in identifying hits if the Glu208 was represented in the conformation in which it is rotated toward the S2 pocket,[49] such as observed in 1AIM (conformation A), while no hits were found in docking to 1ME3 structure, in which the Glu208 side chain is rotated toward solvent. In this study, we again considered both possibilities for Glu208 conformation but obtained better enrichments for structure 1AIM. Therefore, the results obtained with this structure were chosen for the comparison with HTS.

No waters seemed to be conserved among the available structures and therefore prior to docking all waters were removed. Hydrogens were added to standard positions. Matching spheres were generated based on atomic positions of 10 inhibitors from published structures and later modified to be concentrated in the cruzain S2 pocket.

To improve hydrogen bonding complementarity and based on analysis of common hydrogen bonds present in 13 cruzain structures available in the Protein Data Bank (as of July 2007), partial atomic charges were increased by 0.4 in the amide side chain of glutamine 19 (Oε1 and HNε1, HNε2, with the positive charge divided between the two hydrogens and increased by 0.2 in each), in polar atoms of cysteine 25 (O, Sγ, HN, and HSγ), in the amide backbone of aspartate 161 (O and HN), and in polar atoms of glycine 66 (O and HN). This is consistent with similar treatment in earlier prospective docking campaigns from our lab.[4,50] Sampling parameters used were matching tolerance of 1.2 Å and bin sizes of 0.4 Å for both ligand and receptor, with an overlap of 0.3 Å. To accelerate calculations in DOCK, energy potential grids were precalculated using the programs CHEMGRID[28] and Delphi.[51] Multiple conformations and orientations of each ligand were scored based on van der Waals and electrostatic interactions with a penalty for ligand desolvation (M. Mysinger, A.B.D., B.K.S., unpublished).[4,50] The best scoring conformation of each compound was used for ranking the database.

Docking of Compound 27. The 600 conformations of **27** generated by OMEGA (OpenEye Scientific Software, Santa Fe, NM) and used for docking the library were rigidly docked to cruzain, both in the original grids and in grids generated using cruzain coordinates from the determined structure in complex with this compound. Sampling parameters used for single mode runs were matching tolerance of 1.2 Å, bin sizes of 0.4 Å, and bin overlaps of 0.2 Å. Root mean square deviations (rmsd) were calculated between each generated pose and the crystallographic pose of compound **27**.

The program scoreopt was used to investigate detailed scoring for the crystallographic pose of compound **27** in both

grids used. Scoreopt allows the calculation of electrostatic and van der Waals contributions and the desolvation penalty for each atom in the ligand. The scores for each term in the DOCK3.5.54 scoring function were compared to those for the best ranking pose obtained by the program in the same grids.

Papain Counter-Screen. The 921 detergent-resistant, non-fluorescent top hits obtained from qHTS[13] were clustered based on their 2D structures using Leadscope's structural fingerprint and a Tanimoto coefficient cutoff of 0.7. A total of 149 clusters were obtained, 70 of them containing four or more active compounds. These were further filtered based on potency cutoffs. A total of 199 compounds, including active and inactive members of a filtered set of 47 clusters, plus 35 singletons, were screened in parallel against cruzain and papain. Each compound was tested in seven different concentrations against each enzyme. Screening against papain was performed following the protocol and reaction conditions previously described for cruzain[13] with the following two changes: (1) cysteine, added to the buffer at 5 mM final concentration, was used to maintain papain activity instead of the dithiothreitol employed in the cruzain assay and (2) papain was used at a final concentration of 12 nM in order to obtain adequate assay signal.

Cruzain Inhibition Assays. Cruzain activity was measured by monitoring the cleavage of the fluorogenic substrate Z-Phe-Arg-aminomethylcoumarin (Z-FR-AMC). All cruzain assays were performed in sodium acetate 0.1 M pH 5.5 and in the presence of 5 mM dithiothreitol (DTT). The final concentration of cruzain was 0.4 nM, and the substrate concentration was 2.5 μM (K_m = 2 μM), except for K_i determination, when the Z-FR-AMC varied from 0.31 to 20 μM in 2-fold increments. Assays were conducted in presence of 0.01% Triton X-100, except for evaluation of detergent-sensitivity, when inhibition was compared in 0, 0.01 and 0.1% Triton. Assays were followed for 5 min, and activity was calculated based on initial rates.

For evaluation of time-dependent inhibition, percentages of enzyme inhibition by a compound with or without preincubation with enzyme for 10 min were compared. During the preincubation step, cruzain and compound concentrations were 10-fold higher than in the final assay. In assays performed in the absence of detergent, compounds were always preincubated with cruzain for 5 min to allow small molecule aggregate formation because this was the purpose of these nondetergent assays. Investigation of other mechanisms were typically conducted in the presence of detergent, and here there was no preincubation with enzyme unless compound inhibition was known to be time-dependent. For these known time-dependent inhibitors, 5 min incubation was performed to allow discrimination between time-dependence and detergent-sensitivity. We note that in the initial qHTS, the incubation time with and without detergent was the same.[13]

To determine if cruzain inhibitors were competitive, each compound was tested in at least four concentrations (variable depending on IC_{50} against cruzain) and seven concentrations of Z-FR-AMC (0.31−20 μM, in 2-fold increments). Data was analyzed with Prism 4 (GraphPad), and K_i values were determined from Lineweaver−Burk and Dixon plots.

AmpC β-Lactamase Inhibition. AmpC activity was based on rates of cleavage of the substrate CENTA, measured by monitoring absorbance at 405 nm for 3 min and was calculated based on initial rates. Assays were performed at potassium phosphate 50 mM, pH 7.0, with final concentrations of 1 nM enzyme and 100 μM substrate (K_m = 48 μM). All compounds were tested in the absence of Triton X-100 and in the presence of 0.01% Triton X-100, and AmpC inhibition rates were compared. In the assays in the absence of Triton X-100, the compounds were preincubated with enzyme for 5 min before addition of substrate, whereas there was no preincubation step in the assays in the presence of Triton.

Cruzain Expression, Purification, And Crystallography. Cruzain was expressed and purified in a modified version (Lee, Balouch, and Craik, unpublished results) of a previously published protocol,[52] activated and purified as recently described.[21] Active cruzain was inhibited with *S*-methyl methanethiosulfonate (MMTS), a covalent reversible inhibitor, to prevent self-degradation.

MMTS inhibited cruzain was concentrated to 1 mg/mL in 2 mM bis tris buffer pH 5.8. 5 mM DTT was added to reverse MMTS inhibition, followed by addition of compound **11**. The solution was then concentrated down to 7.5 mg/mL. Crystals were obtained by hanging drop method in a previously described crystallization condition, 0.1 M Tris pH 8.5, 2.0 M $NH_4H_2PO_4$;[21] 2−4 μL drops with various protein:mother liquor ratios (1:1, 1.5:1, 2:1) were set up and seeded with previously obtained crystals. Before cryocooling, crystals were soaked for one day in 200 mM DTT and for 1 h in a 1.4 mM solution of **27** in mother liquour. Crystals were cryocooled in a 25% solution of ethylene glycol in mother liquor containing 1.4 mM **27**. Similar protocols were conducted in cocrystallizations of cruzain with compounds **11**, **4**, **5**, and **29**.

Data collection was performed in frozen crystals in beamline 8.3.1 at the Advanced Light Source (ALS, Lawrence Berkeley Laboratory, CA), using ELVES[53] to determine the data collection strategy. For the cruzain/**27** complex, 200 frames were collected, with 0.5 s exposure and 0.5° oscillations between frames. Reflections were indexed and integrated using Mosflm and scaled using SCALA.[54] The structure was solved by molecular replacement using Phaser, with PDB structure 3I06 as the template. Data refinement was performed using Phenix,[55] and models were built using Coot.[56] In the final model, 84.2% of residues were in the most favored regions in the Ramachandran plot, 15.3% were in additional allowed regions and 0.5% in disfavored regions. PDB accession code 3KKU.

Liquid Chromatography/Mass Spectrometry (LC/MS). Solutions of compounds **11**, **4**, and **5** were prepared in 2 mM Bis Tris pH 5.8, in the presence or absence of 100 nM cruzain. Solutions were examined by LC/MS at several time points (from 30 min to 24 h) to investigate if these compounds were degraded over time and if degradation was catalyzed by cruzain. LC/MS was conducted on a Waters Micromass ZQ in ESI+ mode, equipped with a Waters 2996 photodiode array detector and a Waters Alliance 2795 separations module. Compounds were eluted through an analytical Xterra C-18 column, using a methanol (0.2% formic acid)/water (0.2% formic acid) system, with a linear gradient from 5 to 95% water in 6 min and a flow rate of 1 mL/min. Elution was monitored at 254 nm.

Compound Purity. As previously described,[13] all compounds in the MLSMR library were purchased and their purity was certified by the corresponding vendors. Briefly, the entire screening library (Galapagos Biofocus DPI, South San Francisco, CA) was subjected to purity analysis before plating by using an eight-channel MUX high-throughput parallel chromatographic system (Micromass Ltd., Manchester, UK, and Waters, Milford, MA) and separating the sample on Phenomenex Gemini 5 um C18 column (2 mm × 50 mm). Compounds used in the follow up experiments were reanalyzed for purity via liquid chromatography−mass spectrometry (LCMS). All compounds passed purity criteria (≥95%). For follow up assays at UCSF, compounds **26**, **44**, and **45** were resourced from the NCGC. All other compounds were purchased and that their purity certified as at least 90% (frequently >95%) by their vendors. Among the compounds confirmed as competitive inhibitors, **4**, **5**, and **8** were purchased from Enamine, with at least 90% purity assured by the company. Compounds **27** and **29** were purchased from ChemBridge and IBScreen, respectively, and both were certified >95% pure; for compound **27**, the 1.28 Å X-ray structure, in complex with the cruzain, was consistent with its reported structure.

Ligand-Based Virtual Screening. We screened the MLSMR library against the cruzain reference set using the similarity ensemble approach (SEA).[26] For pairwise molecule comparisons, we used Tanimoto coefficients with both 1024-bit folded

Scitegic ECFP_4 topological fingerprints and 2048-bit folded Daylight fingerprints, each in separate SEA runs, as previously described.[26,57,58] The reference set was composed of 128 cruzain inhibitors. Of those, we obtained 118 unique cruzain inhibitors with $K_i \leq 1$ uM from the ChEMBL_02 database (http://www.ebi.ac.uk/chembldb/) and 10 inhibitors with $IC_{50} < 1$ uM from the Collaborative Drug Discovery database.[5] We processed and canonicalized all cruzain inhibitor and all 239762 unique MLSMR1 compound structures as previously described.[26,57,58] We then compared all hits with E-values $\leq 1 \times 10^{-1}$ to the list of 146 competitive cruzain inhibitors. We chose a particularly weak E-value threshold here to demonstrate that any competitive cruzain inhibitors not found by this ligand-based virtual screen were missed despite a highly permissive search.

Acknowledgment. We thank Julie Zorn for help with mass spectrometry. This research was supported in part by the Molecular Libraries Initiative of the National Institutes of Health Roadmap for Medical Research and by the Intramural Research Program of NHGRI, NIH, by NIH grant GM59957 (to B.K.S.), and by the Sandler Center for Basic Research in Parasitic Diseases (to J.H.M.). We thank OpenEye Scientific Software for software licenses including Omega and OEChem.

Supporting Information Available: Lineweaver−Burk plots for representative compounds for five classes of cruzain competitive inhibitors. Enrichment curves at each stage of mechanistic follow up. Chemical stability and time-dependence cruzain inhibition data. Comparison between cruzain structure used for docking and crystal structure of cruzain/**27** complex. Superposition of conformation of **27** in complex with cruzain and closest conformation found by docking. Follow up of HTS hits ranked among the top 1% of the dock ranked database. DOCK ranking and experimental follow up of compound **4** analogues (cluster 44). Follow up of clusters selective for cruzain. Potential qHTS false negatives prioritized for testing by docking. Comparison of DOCK scores for crystallographic and DOCK poses of compound **27**. Synthesis and in vitro activity of analogues of compound **11**. This material is available free of charge via the Internet at http://pubs.acs.org.

References

(1) Stockwell, B. R. Exploring biology with small organic molecules. *Nature* **2004**, *432*, 846–854.
(2) Lipinski, C.; Hopkins, A. Navigating chemical space for biology and medicine. *Nature* **2004**, *432*, 855–861.
(3) Stahl, M.; Rarey, M. Detailed analysis of scoring functions for virtual screening. *J. Med. Chem.* **2001**, *44*, 1035–1042.
(4) Babaoglu, K.; Simeonov, A.; Irwin, J. J.; Nelson, M. E.; Feng, B.; Thomas, C. J.; Cancian, L.; Costi, P.; Maltby, D. A.; Jadhav, A.; Inglese, J.; Austin, C.; Shoichet, B. K. Comprehensive mechanistic analysis of hits from high-throughput and docking screens against β-lactamase. *J. Med. Chem.* **2008**, *51*, 2502–2511.
(5) Doman, T. N.; McGovern, S. L.; Witherbee, B. J.; Kasten, T. P.; Kurumbail, R.; Stallings, W. C.; Connolly, D. T.; Shoichet, B. K. Molecular docking and high-throughput screening for novel inhibitors of protein tyrosine phosphatase-1B. *J. Med. Chem.* **2002**, *45*, 2213–2221.
(6) Polgar, T.; Baki, A.; Szendrei, G. I.; Keseru, G. M. Comparative virtual and experimental high-throughput screening for glycogen synthase kinase-3β inhibitors. *J. Med. Chem.* **2005**, *48*, 7946–7959.
(7) Bologa, C. G.; Revankar, C. M.; Young, S. M.; Edwards, B. S.; Arterburn, J. B.; Kiselyov, A. S.; Parker, M. A.; Tkachenko, S. E.; Savchuck, N. P.; Sklar, L. A.; Oprea, T. I.; Prossnitz, E. R. Virtual and biomolecular screening converge on a selective agonist for GPR30. *Nature Chem. Biol.* **2006**, *2*, 207–212.
(8) Edwards, B. S.; Bologa, C.; Young, S. M.; Balakin, K. V.; Prossnitz, E. R.; Savchuck, N. P.; Sklar, L. A.; Oprea, T. I. Integration of virtual screening with high-throughput flow cytometry to identify novel small molecule formylpeptide receptor antagonists. *Mol. Pharmacol.* **2005**, *68*, 1301–1310.
(9) Fara, D. C.; Oprea, T. I.; Prossnitz, E. R.; Bologa, C. G.; Edwards, B. S.; Sklar, L. A. Integration of virtual and physical screening. *Drug Discovery Today: Technol.* **2006**, *3*, 377–385.
(10) Feng, B. Y.; Simeonov, A.; Jadhav, A.; Babaoglu, K.; Inglese, J.; Shoichet, B. K.; Austin, C. P. A high-throughput screen for aggregation-based inhibition in a large compound library. *J. Med. Chem.* **2007**, *50*, 2385–2390.
(11) Engel, J. C.; Doyle, P. S.; Hsieh, I.; McKerrow, J. H. Cysteine protease inhibitors cure an experimental *Trypanosoma cruzi* infection. *J. Exp. Med.* **1998**, *188*, 725–734.
(12) Inglese, J.; Auld, D. S.; Jadhav, A.; Johnson, R. L.; Simeonov, A.; Yasgar, A.; Zheng, W.; Austin, C. P. Quantitative high-throughput screening: a titration-based approach that efficiently identifies biological activities in large chemical libraries. *Proc. Natl. Acad. Sci. U.S.A.* **2006**, *103*, 11473–11478.
(13) Jadhav, A.; Ferreira, R. S.; Klumpp, C.; Mott, B. T.; Austin, C. P.; Inglese, J.; Thomas, C. J.; Maloney, D. J.; Shoichet, B. K.; Simeonov, A. Quantitative Analyses of Aggregation, Autofluorescence, and Reactivity Artifacts in a Screen for Inhibitors of a Thiol Protease. *J. Med. Chem.* **2010**, *53*, 37–51.
(14) Brak, K.; Doyle, P. S.; McKerrow, J. H.; Ellman, J. A. Identification of a new class of nonpeptidic inhibitors of cruzain. *J. Am. Chem. Soc.* **2008**, *130*, 6404–6410.
(15) Gillmor, S. A.; Craik, C. S.; Fletterick, R. J. Structural determinants of specificity in the cysteine protease cruzain. *Protein Sci.* **1997**, *6*, 1603–1611.
(16) Irwin, J. J.; Shoichet, B. K. ZINC—a free database of commercially available compounds for virtual screening. *J. Chem. Inf. Model.* **2005**, *45*, 177–182.
(17) Lorber, D. M.; Shoichet, B. K. Hierarchical docking of databases of multiple ligand conformations. *Curr. Top. Med. Chem.* **2005**, *5*, 739–749.
(18) Wei, B. Q.; Baase, W. A.; Weaver, L. H.; Matthews, B. W.; Shoichet, B. K. A model binding site for testing scoring functions in molecular docking. *J. Mol. Biol.* **2002**, *322*, 339–355.
(19) Simeonov, A.; Jadhav, A.; Thomas, C. J.; Wang, Y.; Huang, R.; Southall, N. T.; Shinn, P.; Smith, J.; Austin, C. P.; Auld, D. S.; Inglese, J. Fluorescence spectroscopic profiling of compound libraries. *J. Med. Chem.* **2008**, *51*, 2363–2371.
(20) Huth, J. R.; Mendoza, R.; Olejniczak, E. T.; Johnson, R. W.; Cothron, D. A.; Liu, Y.; Lerner, C. G.; Chen, J.; Hajduk, P. J. ALARM NMR: a rapid and robust experimental method to detect reactive false positives in biochemical screens. *J. Am. Chem. Soc.* **2005**, *127*, 217–224.
(21) Mott, B. T.; Ferreira, R. S.; Simeonov, A.; Jadhav, A.; Ang, K. K.; Leister, W.; Shen, M.; Silveira, J. T.; Doyle, P. S.; Arkin, M. R.; McKerrow, J. H.; Inglese, J.; Austin, C. P.; Thomas, C. J.; Shoichet, B. K.; Maloney, D. J. Identification and Optimization of Inhibitors of Trypanosomal Cysteine Proteases: Cruzain, Rhodesain, and TbCatB. *J. Med. Chem.* **2010**, *53*, 52–60.
(22) McGovern, S. L.; Caselli, E.; Grigorieff, N.; Shoichet, B. K. A common mechanism underlying promiscuous inhibitors from virtual and high-throughput screening. *J. Med. Chem.* **2002**, *45*, 1712–1722.
(23) Bryant, C.; Kerr, I. D.; Debnath, M.; Ang, K. K.; Ratnam, J.; Ferreira, R. S.; Jaishankar, P.; Zhao, D.; Arkin, M. R.; McKerrow, J. H.; Brinen, L. S.; Renslo, A. R. Novel non-peptidic vinylsulfones targeting the S2 and S3 subsites of parasite cysteine proteases. *Bioorg. Med. Chem. Lett.* **2009**, *19*, 6218–6221.
(24) Verdonk, M. L.; Berdini, V.; Hartshorn, M. J.; Mooij, W. T.; Murray, C. W.; Taylor, R. D.; Watson, P. Virtual screening using protein−ligand docking: avoiding artificial enrichment. *J. Chem. Inf. Comput. Sci.* **2004**, *44*, 793–806.
(25) Tirado-Rives, J.; Jorgensen, W. L. Contribution of Conformer Focusing to the Uncertainty in Predicting Free Energies for Protein−Ligand Binding. *J. Med. Chem.* **2006**, *49*, 5880–5884.
(26) Keiser, M. J.; Roth, B. L.; Armbruster, B. N.; Ernsberger, P.; Irwin, J. J.; Shoichet, B. K. Relating protein pharmacology by ligand chemistry. *Nature Biotechnol.* **2007**, *25*, 197–206.
(27) Shoichet, B. K.; Leach, A. R.; Kuntz, I. D. Ligand solvation in molecular docking. *Proteins* **1999**, *34*, 4–16.
(28) Meng, E. C.; Shoichet, B. K.; Kuntz, I. D. Automated docking with grid-based energy evaluation. *J. Comput. Chem.* **1992**, *13*, 505–524.
(29) Shoichet, B. K. Interpreting steep dose−response curves in early inhibitor discovery. *J. Med. Chem.* **2006**, *49*, 7274–7277.
(30) Walters, W. P.; Ajay; Murcko, M. A. Recognizing molecules with drug-like properties. *Curr. Opin. Chem. Biol.* **1999**, *3*, 384–387.
(31) Walters, W. P.; Namchuk, M. A guide to drug discovery. Designing screens: how to make your hits a hit. *Nature Rev. Drug Discovery* **2003**, *2*, 259–266.
(32) Rishton, G. M. Reactive compounds and in vitro false positives in HTS. *Drug Discovery Today* **1997**, *2*, 382–384.

(33) Roche, O.; Schneider, P.; Zuegge, J.; Guba, W.; Kansy, M.; Alanine, A.; Bleicher, K.; Danel, F.; Gutknecht, E. M.; Rogers-Evans, M.; Neidhart, W.; Stalder, H.; Dillon, M.; Sjögren, E.; Fotouhi, N.; Gillespie, P.; Goodnow, R.; Harris, W.; Jones, P.; Taniguchi, M.; Tsujii, S.; von der Saal, W.; Zimmermann, G.; Schneider, G. Development of a virtual screening method for identification of "frequent hitters" in compound libraries. *J. Med. Chem.* **2002**, *45*, 137–142.
(34) Huth, J. R.; Sun, C.; Sauer, D. R.; Hajduk, P. J. Utilization of NMR-derived fragment leads in drug design. *Methods Enzymol.* **2005**, *394*, 549–571.
(35) Ryan, A. J.; Gray, N. M.; Lowe, P. N.; Chung, C. W. Effect of detergent on "promiscuous" inhibitors. *J. Med. Chem.* **2003**, *46*, 3448–3451.
(36) Liu, H.; Wang, Z.; Regni, C.; Zou, X.; Tipton, P. A. Detailed kinetic studies of an aggregating inhibitor: inhibition of phosphomannomutase/phosphoglucomutase by Disperse Blue 56. *Biochemistry* **2004**, *27*, 8662–8669.
(37) Giannetti, A. M.; Koch, B. D.; Browner, M. F. Surface plasmon resonance based assay for the detection and characterization of promiscuous inhibitors. *J. Med. Chem.* **2008**, *51*, 574–580.
(38) Yang, C. Y.; Sun, H.; Chen, J.; Nikolovska-Coleska, Z.; Wang, S. Importance of ligand reorganization free energy in protein−ligand binding affinity prediction. *J. Am. Chem. Soc.* **2009**, *131*, 13709–13721.
(39) Sherman, W.; Day, T.; Jacobson, M. P.; Friesner, R. A.; Farid, R. Novel procedure for modeling ligand/receptor induced fit effects. *J. Med. Chem.* **2006**, *49*, 534–553.
(40) Schnecke, V.; Swanson, C. A.; Getzoff, E. D.; Tainer, J. A.; Kuhn, L. A. Screening a peptidyl database for potential ligands to proteins with side-chain flexibility. *Proteins* **1998**, *33*, 74–87.
(41) Claussen, H.; Buning, C.; Rarey, M.; Lengauer, T. FlexE: efficient molecular docking considering protein structure variations. *J. Mol. Biol.* **2001**, *308*, 377–395.
(42) Cavasotto, C. N.; Kovacs, J. A.; Abagyan, R. A. Representing receptor flexibility in ligand docking through relevant normal modes. *J. Am. Chem. Soc.* **2005**, *127*, 9632–9640.
(43) Michel, J.; Tirado-Rives, J.; Jorgensen, W. L. Prediction of the water content in protein binding sites. *J. Phys. Chem. B* **2009**, *113*, 13337–13346.
(44) Huang, N.; Shoichet, B. K. Exploiting ordered waters in molecular docking. *J. Med. Chem.* **2008**, *51*, 4862–4865.
(45) Barillari, C.; Taylor, J.; Viner, R.; Essex, J. W. Classification of water molecules in protein binding sites. *J. Am. Chem. Soc.* **2007**, *129*, 2577–2787.
(46) Young, T.; Abel, R.; Kim, B.; Berne, B. J.; Friesner, R. A. Motifs for molecular recognition exploiting hydrophobic enclosure in protein−ligand binding. *Proc. Natl. Acad. Sci. U.S.A.* **2007**, *104*, 808–813.
(47) Teague, S. J.; Davis, A. M.; Leeson, P. D.; Oprea, T. The design of leadlike combinatorial libraries. *Angew. Chem., Int. Ed. Engl.* **1999**, *38*, 3743–3748.
(48) Gillmor, S. A.; Craik, C. S.; Fletterick, R. J. Structural determinants of specificity in the cysteine protease cruzain. *Protein Sci.* **1997**, *6*, 1603–1611.
(49) Ferreira, R. S.; Bryant, C.; Ang, K. K.; McKerrow, J. H.; Shoichet, B. K.; Renslo, A. R. Divergent Modes of Enzyme Inhibition in a Homologous Structure−Activity Series. *J. Med. Chem.* **2009**, *52*, 5005–5008.
(50) Kolb, P.; Rosenbaum, D. M.; Irwin, J. J.; Fung, J. J.; Kobilka, B. K.; Shoichet, B. K. Structure-based discovery of β2-adrenergic receptor ligands. *Proc. Natl. Acad. Sci. U.S.A.* **2009**, *106*, 6843–6848.
(51) Gilson, M. K.; Honig, B. H. Calculation of electrostatic potentials in an enzyme active site. *Nature* **1987**, *330*, 84–86.
(52) Eakin, A. E.; McGrath, M. E.; McKerrow, J. H.; Fletterick, R. J.; Craik, C. S. Production of crystallizable cruzain, the major cysteine protease from *Trypanosoma cruzi*. *J. Biol. Chem.* **1993**, *268*, 6115–8.
(53) Holton, J.; Alber, T. Automated protein crystal structure determination using ELVES. *Proc. Natl. Acad. Sci. U.S.A.* **2004**, *101*, 1537–1542.
(54) Collaborative Computational Project, N. The CCP4 suite: programs for protein crystallography. *Acta Crystallogr, Sect. D: Biol. Crystallogr.* **1994**, *50*, 760−763.
(55) Adams, P. D.; Grosse-Kunstleve, R. W.; Hung, L.-W.; Ioerger, T. R.; McCoy, A. J.; Moriarty, N. W.; Read, R. J.; Sacchettini, J. C.; Sauter, N. K.; Terwilliger, T. C. PHENIX: building new software for automated crystallographic structure determination. *Acta Crystallogr., Sect. D: Biol. Crystallogr.* **2002**, 58.
(56) Emsley, P.; Cowtan, K. Coot: model-building tools for molecular graphics. *Acta Crystallogr., Sect. D: Biol. Crystallogr.* **2004**, *60*, 2126–2132.
(57) Hert, J.; Keiser, M. J.; Irwin, J. J.; Oprea, T. I.; Shoichet, B. K. Quantifying the relationships among drug classes. *J. Chem. Inf. Model.* **2008**, *48*, 755–765.
(58) Keiser, M. J.; Vincent, S.; Irwin, J. J.; Laggner, C.; Abbas, A. I.; Hufeisen, S. J.; Jensen, N. H.; Kuijer, M. B.; Matos, R. C.; Tran, T. B.; Whaley, R.; Glennon, R. A.; Hert, J.; Thomas, K. L. H.; Edwards, D. D.; Shoichet, B. K.; Roth, B. L. Predicting new molecular targets for known drugs. *Nature* **2009**, *462*, 175–181.
(59) DeLano, W. L. *The Pymol Molecular Graphics System*; DeLano Scientific: San Carlos, CA, 2002.